Journal Pre-proofs

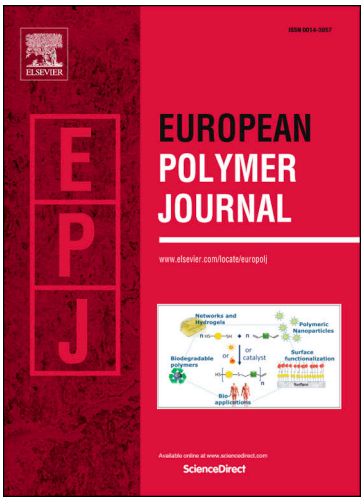


# Single and Dual polymeric sponges for emerging pollutants removal

Chiara Zagni, Sandro Dattilo, Tommaso Mecca, Chiara Gugliuzzo, Andrea A. Scamporrino, Vittorio Privitera, Roberta Puglisi, Sabrina Carola Carroccio

PII: S0014-3057(22)00560-2
DOI: https://doi.org/10.1016/j.eurpolymj.2022.111556
Reference: EPJ 111556

To appear in: *European Polymer Journal*

Received Date: 10 June 2022
Revised Date: 31 August 2022
Accepted Date: 2 September 2022

Please cite this article as: Zagni, C., Dattilo, S., Mecca, T., Gugliuzzo, C., Scamporrino, A.A., Privitera, V., Puglisi, R., Carola Carroccio, S., Single and Dual polymeric sponges for emerging pollutants removal, *European Polymer Journal* (2022), doi: https://doi.org/10.1016/j.eurpolymj.2022.111556

# Single and Dual polymeric sponges for emerging pollutants removal

Chiara Zagni[1*], Sandro Dattilo[2], Tommaso Mecca[3], Chiara Gugliuzzo[2], Andrea A. Scamporrino[2], Vittorio Privitera[4], Roberta Puglisi[2], Sabrina Carola Carroccio[2*].



[1] *Department of Drug and Health Sciences, University of Catania, V.le A. Doria, 95125, Catania, Italy*
[2] *Institute for Polymers, Composites, and Biomaterials CNR-IPCB, Via Paolo Gaifami 18, 95126, Catania, Italy*
[3] *Institute for Biomolecular Chemistry CNR-ICB, Via Paolo Gaifami 18, 95126, Catania, Italy.*
[4] *Institute for Microelectronics and Microstructures CNR-IMM, Via Santa Sofia 64, 95123, Catania, Italy*

Correspondence to: sabrinacarola.carroccio@cnr.it

**Abstract**

A platform of polymeric cryogels based on methacrylic acid (C-mA) meglumine (C-megl), lysine (C-lys), and 2-hydroxy ethyl methacrylate (C-ph), as well as a combination thereof having both negatively and positively charged moieties, have been synthesized and used to efficiently remove emerging contaminants from water. Their peculiar properties in sequestering antibiotics (Levofloxacin, Ampicillin, Doxycycline), anti-inflammatory (Piroxicam), antifungal (Fluconazole), anti-parasite (Moxidectin), pesticides (2,4D) and dyes (Thymol blue, Methylene Violet) were tested taking into account their ionic nature in solution. The adsorption experiments performed in batches at different pH and pollutant concentrations have demonstrated the outstanding ability of these macroporous soft systems in complexing molecules by the instauration of various binding forces, also in the presence of inorganic species such as arsenic (as arseniate). In addition, it was demonstrated as the novel dual-material, *ad-hoc* synthesized by using opposite charge cryogels can simultaneously remove antagonist dyes in a single and fast cycle. Besides, a quasi-total release of the target molecules was achieved by changing pH, allowing the regeneration of the macroporous sponges for multiple re-uses without losing their performance. The latter peculiar feature may be adopted for drug delivery applications since the release can be modulated and programmed by a specific pH stimulus.

**Keywords**: cryogel, polymer, emerging pollutant, pharmaceutical, antibiotic, dye, 2,4 D, adsorption, hydrogel, drug delivery.

## 1. Introduction

Removal of emerging pollutants from water, such as pharmaceuticals, pesticides, and dyes, represents one of the most relevant challenges of this millennium. Among the emerging organic

contaminants (EOCs), pharmaceuticals represent an insidious concern due to the insurgence of multi-drug resistance microorganisms.[1,2] Diverse studies have been reported on the potential toxicity of EOCs. Many belong to these matrices' antibiotic, analgesic/anti-inflammatory, antifungal, antiparasitic, pesticide, and dye groups.



In light of this, investigating their metabolisms and methods to avoid their contamination effects has recently become a central topic for the scientific community.[4]

Indeed, pharmaceuticals and pesticides are the most common emerging pollutants introduced into the soil and aquatic systems due to animal waste, freshwater aquaculture waste, and domestic, hospital, and industrial waste.[5]

However, the wastewater treatment plants (WWTPs), designed to remove oxygen demand pollutants, are only moderately effective in eliminating pharmaceuticals, with less than 10% remediation efficiency.[6] As a result, such dangerous molecules are finally re-immitted into the water bodies. As far as it is concerned, the complete removal of EOCs is still a "great challenge".[7,8]

The growing environmental awareness of protecting our ecosystem has significantly increased the scientific efforts to envisage novel strategies for the remediation and prevention of contaminated sites. Among these, technologies based on adsorption, advanced oxidation processes (AOPs), biological technologies, separation processes, and multiple-treatment procedures have received relevant attention.[9] Mainly, adsorption-based techniques are highly considered for removing EOCs because of their flexibility, low cost, and easy application. [10–13]

In the present study, we focused on the adsorption of EOCs, of selected contaminants reported in **Table 1,** by using polymeric adsorbent cryogels based on functional acrylic and vinyl-benzylic monomers (**Table 2**).

**Table 1**. Selected pollutants*

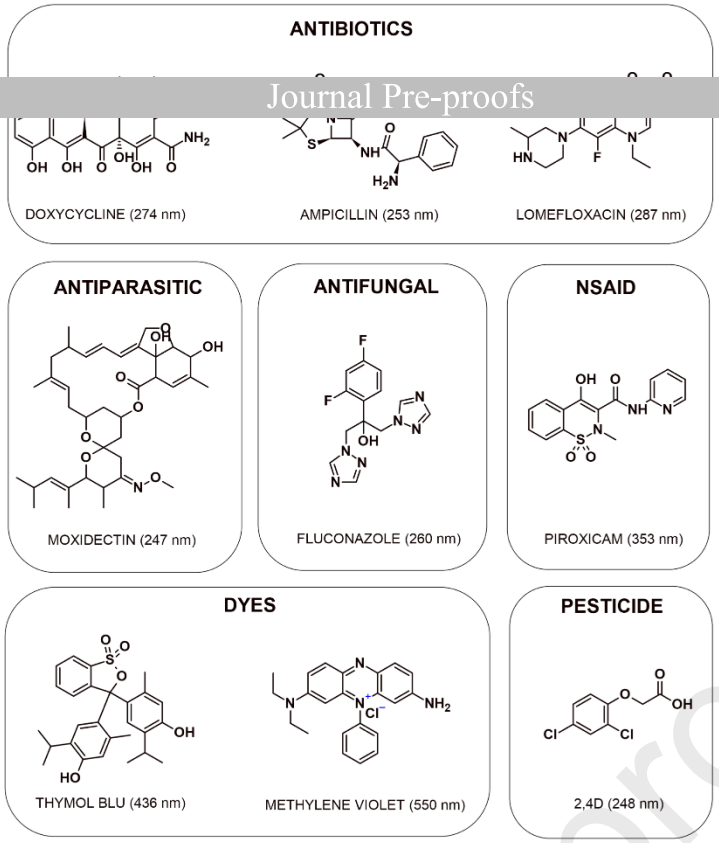


*absorbtion wavelengths in brakets



Specifically, we selected as target molecules: lomefloxacin (Lome), ampicillin (Amp), and doxycycline (Doxi), the non-steroidal anti-inflammatory (NSAIDs), piroxicam (Piro), the antimycotic fluconazole (Fluco), the antiparasitic Moxidectin (Moxi). They are all commonly used and detected in superficial waters.[14–16]

Lome belongs to the amphoteric class of fluoroquinolone (FQs).[17] In some countries, it is used in aquaculture to prevent disease in aquatic species, although, in Europe, it was no longer allowed.[18]

Amp is a representative of the β-lactam antibiotics that accounts for over 65% of the world antibiotic market.[19] In contrast, Doxi is a tetracycline released into the environment primarily through its use as a veterinary antibiotic,[20] and subsequently discharged via the animals' excretion. Similarly, Moxi is an antiparasitic drug used worldwide to treat cattle whose excretions are used as fertilizer.[21] Its toxicity to the marine environment was demonstrated over zebrafish embryos models.[22]

The Piro treats inflammations associated with arthritis and other musculoskeletal conditions.[23] The consumption of this drug reaches a value of tons per year, so it is found in the wastewater in the

amount of ng/L or lg/L, exhibiting a high environmental toxicity.[24] Finally, Fluco belongs to fungicides used in agriculture and human medicine.[25]

Together with the emerging pharmaceutical pollutants, we also considered the contamination derived from well-recognized sources such as the pesticide 2,4-Dichlorophenylacetic acid (2,4-D), the dyes methylene violet (M-Viol) and thymol blue (T-Blue).[27]



Specifically, M-Viol is widely used in the textile industries and also known as crystal violet for medical uses.

Polymeric hydrogels are widely studied for environmental and drug delivery applications[28–30] due to the peculiar chemical and/or physical complexation properties that can be tuned to satisfy the removal or release of specific species.

Among this class of adsorbents, we focused our attention on "cryogels" produced in various shapes and sizes at subzero temperatures with a low cost and toxic-free procedure since water is used as a solvent. Differently from the most renowned aerogels,[31–33] cryogels are characterized by macroporous connected systems with dimensions comprised from sub-micrometer to hundred micrometers, with improved mechanical and osmotic stabilities. Such polymeric sponges, able to restore their original form after compression, can make the difference in these application areas. Indeed, the super-absorbent property allows rapid access to all active sites, therefore pollutants are readily sequestered and stably linked to the soft-bulk.[34-37] If used with heterogeneous solutions, the large pores allow limited flow resistance and pores obstruction. In this view, it was recently demonstrated that cryogels can be an attractive freestanding platform for the removal of inorganic pollutants in aqueous media such as Cd, Ni, As and Cr.[38–40,51]

However, literature lacks to report their use to remove emerging pollutants from water, and particularly towards pharmaceuticals. In this view, benefits introduced by cryogels could be proficiently extended to the adsorption of these class of contaminants directly at the output of wastewater treatment plant of pharmaceutical industries.

To this aim, as novelty we proposed herein the use of cryogels based on meglumine (C-megl), lysine (C-lys), methacrylic acid (C-mA), and 2-hydroxyethyl methacrylate (C-ph) for the capture of all selected target molecules. Based on uptake results, a new dual sponge formed by C-mA and C-megl was specifically designed to adsorb different species present in water in a single and rapid step.

Adsorption capacity, selectivity, recyclability, and the release of the adsorbates as a function of pH were herein reported and discussed.

To the best of our knowledge, cryogels able to adsorb pharmaceuticals and selectively remove species with opposite charges (i.e. anionic and cationic drugs) from water, concentrating and releasing the target species on demand, were not yet investigated.



## 2. Experimental

### 2.1 Materials

2-Hydroxyethyl methacrylate (HEMA), N, N'-methylene-bisacrylamide (MBAA), ammonium persulfate (APS), tetramethyl-ethylene-diamine (TEMED), Ampicillin sodium salt, ethanol (99.9%), hydrochloric acid (37%), DMSO (99.7%), methanol (≥99.9%), trifluoroacetic acid (TFA), dimethylformamide anhydrous (DMF), *N, N*'-diisopropyl carbodiimide (DIC), 4-dimethyl aminopyridine (DMAP), 2,4-Dichlorophenoxyacetic acid solution (2,4D), Moxidectin, methylene violet, and thymol blue sodium salt were all purchased from Sigma-Aldrich and used as received. Boc-Lys(Boc)-OH DCHA was obtained from Novabiochem (Hohenbrunn, Germany). (4-Vinyl-benzyl)-N-methyl-D-glucamine, pHEMA-lys, and metacrylic acid criogels were synthesized in our laboratory. Lomefloxacin chlorohydrate, Fluconazole, Piroxicam, and Doxycycline Hyclate were kindly obtained (assigned purity > 99%) from Medivis srl. A Milli-Q water purification system produced the deionized water.

### 2.2 Synthesis of Cryogels

C-ph cryogel was obtained using a monomer (HEMA and MBAA) solution (10% w/w) in water with a molar ratio of 6:1 and of APS/TEMED (1% (w/w) of the total monomer concentration).[41] Subsequently, it was functionalized with Boc-Lys(Boc)-OH DCHA using DIC and DMAP and washed with DMF/$CH_2Cl_2$ at a ratio of 2:1, 1:2, and finally with pure $CH_2Cl_2$ to obtain pHEMA-*N, N*'-di-Boc-L-lysine. Deprotection of *N*-Boc was carried out using TFA to obtain C-lys.[42]

C-mA has been synthesized by polymerizing and cross-linking methacrylic acid by *N*, *N*'-methylene bisacrylamide (MBAA) in a molar ratio of 5/1 in water at subzero temperature.[43]

C-megl was obtained by cryo-polymerization of meglumine-based monomer using MBAA as crosslinker (molar ratio 1/6 compared to the moles of monomer) as reported by Mecca *et al*..[39]

The dual polymeric cryogel containing both C-megl and C-mA was synthesized as follows: a solution of meglumine based monomer and MBAA as crosslinker with a molar ratio of 6/1 and APS/TEMED as radical initiators was mixed and cooled down to –15°C allowing the solution to freeze for about 4 minutes. A freshly prepared solution of methacrylic acid and MBAA in a molar ratio of 5/1 was

then cooled down to 0°C and a mixture of APS/TEMED was added to start the polymerization. The solution was pre-cooled at about T = -10°C then added to the frozen sample and allowed to freeze. After 24 hours, the sample was tawed to obtain the "*dual*" cryogel. The procedure is schematically



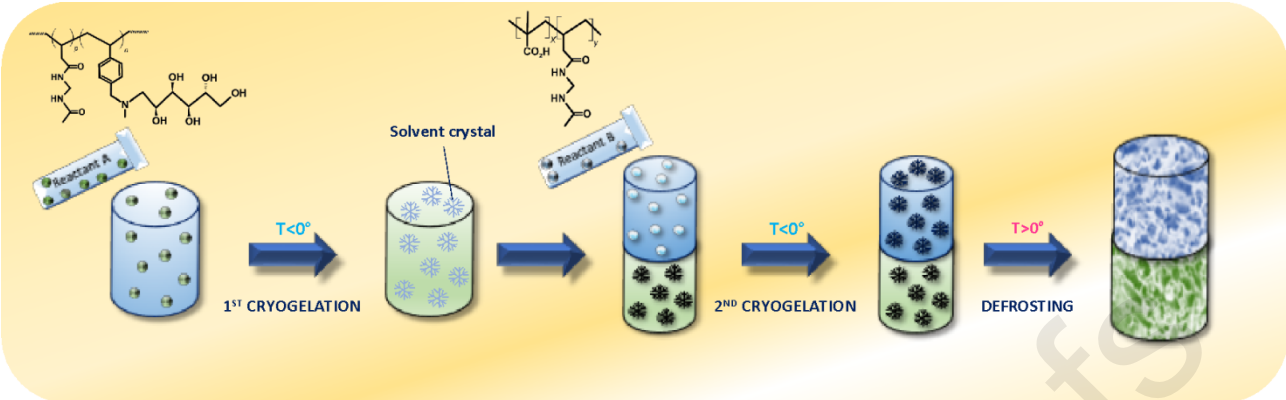


**Figure 1.** Schematic representation of synthesis employed for the 'dual' systems.

## 2.2 Cryogels characterization

The polymers were characterized by various techniques to determine their physico-chemical properties as well as their adsorption and release abilities.

FTIR analyses in the 4000–400 $cm^{-1}$ region were obtained using FTIR System 2000 (Perkin-Elmer, Waltham, MA, USA) and KBr as media.

The UV-VIS spectra were acquired by a Spectrometer Lambda 45 (Perkin-Elmer, Waltham, MA, USA

The thermal stability of the samples was investigated by thermogravimetric analysis (TGA) using a thermogravimetric apparatus (TA Instruments Q500) under a nitrogen atmosphere (flow rate 60 mL/min) and a heating rate of 10 °C/min, from 40 °C to 800 °C. Samples weighted *ca* 5 mg. The weight loss percentage was determined by TGA.

Scanning electron microscopy (SEM) Phenomenex microscope was used to study the morphology of the macroporous gels. Dried samples were cut into thin discs (1–2 mm thick) and sputtered with gold (<10 nm) to confer conductivity. The data were acquired and processed using Phenom Porometric 1.1.2.0 (Phenom-World BV, Eindhoven, The Netherlands).

Swelling tests were performed to estimate the water uptake capability of prepared sponges as described in a previous paper.[32,35] Inductively coupled plasma mass spectrometry (ICP-MS) Nexion 300 X was used to determine the chelating properties versus Arsenic of C-Megl in presence of an organic dye. The standard procedure was reported previously.[44]

The pH at the point zero charge (pHzc) of C-mA, was calculated by pH zero drift method as reported in literature.[45] The carboxyl and amine chlorohydrate contents were determined by titration as reported by Yuan *et al.* obtaining 8.55 mmol/g and 2,59 mmol/g of active monomers for C-mA and C-megl, respectively.



Compression tests of synthesized cryogels were performed using a Thermo Scientific RS6000 rotational rheometer in uniaxial compression mode.

### 2.3 Adsorption experiments

Batch experiments were performed to study the sorption and desorption kinetics of the selected pharmaceuticals. Stock solutions with a concentration of 500 ppm of ampicillin, lomefloxacin, M-Viol and Fluco were prepared by using Milli-Q water. The Piro and Moxi solutions with a concentration of 1000 ppm were prepared in DMSO, whereas the 2,4D and T-Blue 10.000 ppm solution were prepared in methanol. Solutions were then diluted with the appropriate amount of water and the pH was adjusted to 6.5, prior to their use for the adsorption tests. To this purpose, 5 mg of each adsorbent was added to 5 mL of adsorbate solutions and shaken in an incubator shaker at 150 rpm at 25 ± 0.5 °C for 24h. Solutions of Piro, Lome and Moxi at 25, 50 and 100 ppm were prepared to this purpose. After contact (5, 10, 15, 30, 60, 180 min, 24 h), a fixed aliquot of the solution was filtered. For the soluble compounds T-Blue and M-Viol, concentrations up to 900 ppm were tested. Whereas solutions up to 800 ppm were prepared to study Langmuir and Freundlich isotherms model of 2, 4 D adsorption. The residual contaminant concentration was measured by UV-Vis spectrophotometer at the characteristic $\lambda_{max}$ reported in **Table 1**. UV Calibration curves for all samples were reported in the **Fig S1.**

### 2.4 pH effect on the desorption

In order to evaluate drug release, materials were placed in a solution whose pHs were adjusted to the desired pH value (1, 3, 4.5 and 9) by adding the appropriate amount of 1M HCl or NaOH. UV measurements were carried out at a fixed time intervals (15, 45, 120, 245 min, and 24h) to check the effectiveness of the pH-responsive release of the drugs.

To verify the regeneration efficiency, C-megl and C-lys were poured into pollutants solution at a concentration of 25 ppm for 245 min. Then, they were washed with a solution of HCl 1 M. The pH

was restored to its initial value by washing the adsorbents with Millipore water. This procedure was repeated for four times measuring the adsorption capacity after each regeneration cycle.



## RESULTS AND DISCUSSION

This work aims to design a cryogel platform that can be used to effectively adsorb organic contaminants, eliminating them from water bodies. In light of this, depending on the nature of pollutants, this study can help to solve environmental issues derived from emerging contaminants. Since electrostatic interaction is the main driving force governing adsorption and release, cryogels were synthesized to interact both with positive and negative charges. In addition, the 2-hydroxyethyl methacrylate (C-ph) based cryogel was polymerized as a neutral reference. Indeed, interactions such as hydrogen bonds and π-π staking may also influence the adsorption process.

Cryogels based on meglumine in its ammonium chloride form (C-megl) and lysine (C-lys) possess basic properties at neutral pH due to the presence of the amine group.[39,41] Megl is characterized by a pKa close to 9.5 and an ammonium content of 2.59 mmol/g; this implies that amine groups are almost entirely protonated near neutrality. The same also applies to Lys that has a pKa of 8.95. Thus, from acid to neutral regions, both cryogels likely attract negatively charged molecules. A pH increase is paralleled by a significant decrease of the adsorption; the progressive loss of positively charged sites resulting from the deprotonation of active sites weakens the attractive interaction between the cryogel and the molecules of interest that are negatively charged. Interestingly, a reversal of the attractive interactions may be exploited to release pharmaceuticals and other pollutants from loaded cryogels; this may be achieved simply by controlling the pH of the solution.

The methacrylic based cryogel (C-mA) with a content of carboxylic moieties of 8.55 mmol/g, is negatively charged at pH 6.5 since the pKa of anchoring sites are lower than 5 and the pHz herein calculated is 5.9. This means that at pH values in the conditions used by us, the active sites are deprotonated and mainly interact with positively charged molecules.[46,47] Our value for the C-mA is higher than that obtained for similar polymers with carboxylate moieties (45); the data obtained for C-Megl cannot be compared with literature data since, to the best of our knowledge, no data for polymers with ammonium pendants have been reported in literature so far.

Obviously, also in the case of C-mA, the adsorption and release of the molecules can be triggered and fine-tuned by changing the pH values of the solution. Following the desorption, the cryogel may be used for a new cycle.

**Table 2.** Cryogels investigated.



| | Reagent | Yield | Charge* |
|---|---|---|---|
| C-megl | 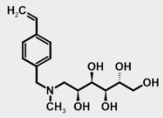 | 70/80% | Positive |
| C-lys | 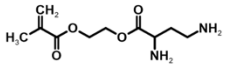 | 85% | Positive |
| C-mA |  | 80% | Negative |
| C-ph | 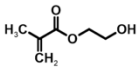 | 73% | Neutral |

* Charge at pH=6.5

All cryogels were characterized from the chemical-physical point of view. FT-IR spectra (Fig. S2) supports the formation of entities whose thermal properties are reported in **Tab S1** (thermograms in Fig S3). FT-IR spectra of the four polymeric materials were compared with the parent monomers in **Tab. 2**.[39,48–50] Our results show the disappearance of the pattern of the typical signal ascribed to methylene (-C=C) groups of the monomers in the range 1000-800 $cm^{-1}$ (see SI, Figure S2) and support the formation of the polymeric sponge. The polymerization yields range from 73 to 90% depending on the monomer used (**Table 2**).

The interconnected macroporous structures of cryogels entailed the formation of fast water diffusion pathways allowing a rapid achievement of the equilibrium adsorption process. [39,41] The swelling tests revealed high water uptake for all materials (Fig. S4a), although C-mA is characterized by a higher swelling value than other samples. After squeezing, cryogels release the retained water and can be subjected to re-adsorption. Adsorption properties did not change over the number of cycles (usually not less than five) tested in the present work (Fig. S4b).

Morphological analyses are shown in **Figure 2** (a-d). Micrographs show that all materials have the typical macroporous structure; pore dimensions range from 24-98, 23-72, 24-84 and 24-134 µm for C-lys, C-megl, C-mA and C-ph, respectively. The pore distribution, average pore area ratio and circle equivalent diameters are reported in the figure S5 and Table S2.

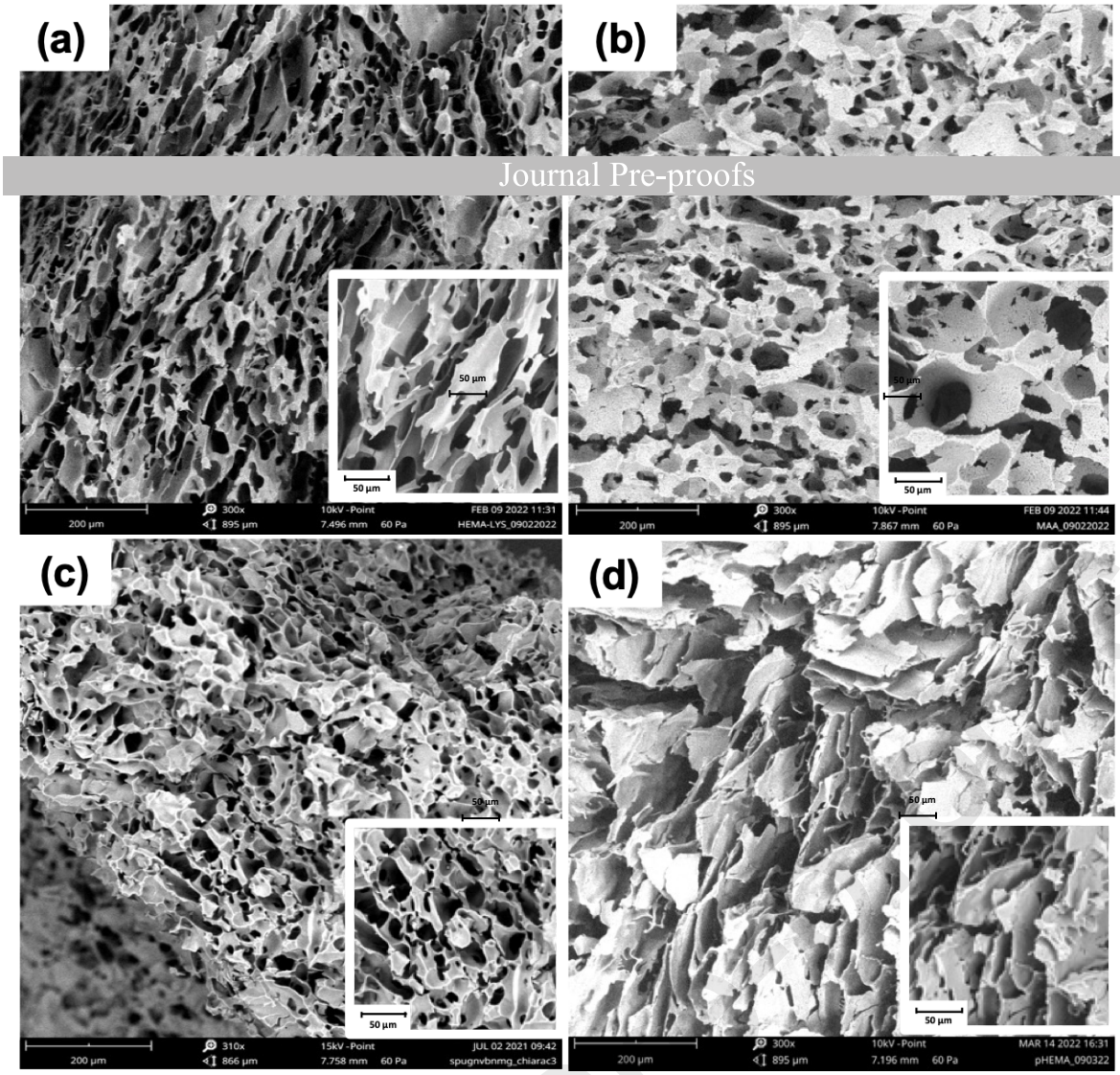


**Figure 2.** SEM images of the Cryogels: (a) C-lys; (b) C-mA; (c) C-megl; (d) C-ph.

**ADSORPTION TESTS**

To evaluate the adsorption properties versus the selected contaminants, C-megl was soaked in the *ad hoc* 'contaminated' water at pH 6.5 (see experimental section), and the pollutants uptake was measured by UV-Vis. Megl derivatives have been previously employed to remove different inorganic components such as Cr (VI), As (IV), and Boron (III).[39,51,52] In the present work we have used the same derivatives to remove the selected polluting organic chemicals listed in **Table 1**. The % of adsorption of the target molecules are reported in **Figure 3** for all the investigated cryogels. C-megl adsorbed Piro, 2,4 D, Moxi and T-blue with outstanding efficiency though C-mA removed Moxi even more efficiently. Since all cryogels (see structures in **Table 1**) adsorbed Moxi, independently from

their charge or structure, it can be reasonably assumed that hydrogen interactions.  are the main driven forces involved in the process.

Piro presents both acidic and basic properties with $pKa_2$ values ranging from 5.3- 5.7.[53] At the pH



megl.

Similarly, both 2,4 D (pKa = 2.73) and T-Blue ( pKa = 1.6 and 8.9) are sequestered from C-megl since they are negatively charged at the pH used.[54]

In particular, the maximum adsorption capacities (Qm) calculated with Langmuir isotherms showed surprising value for 2,4 D (420.45 mg/g) if compared to data reported in the literature for other adsorbent materials (Figure S10, Table S4).[55]

As predictable, the other compounds tested were not adsorbed since they are not negatively charged under the conditions employed (**Figure 3**).

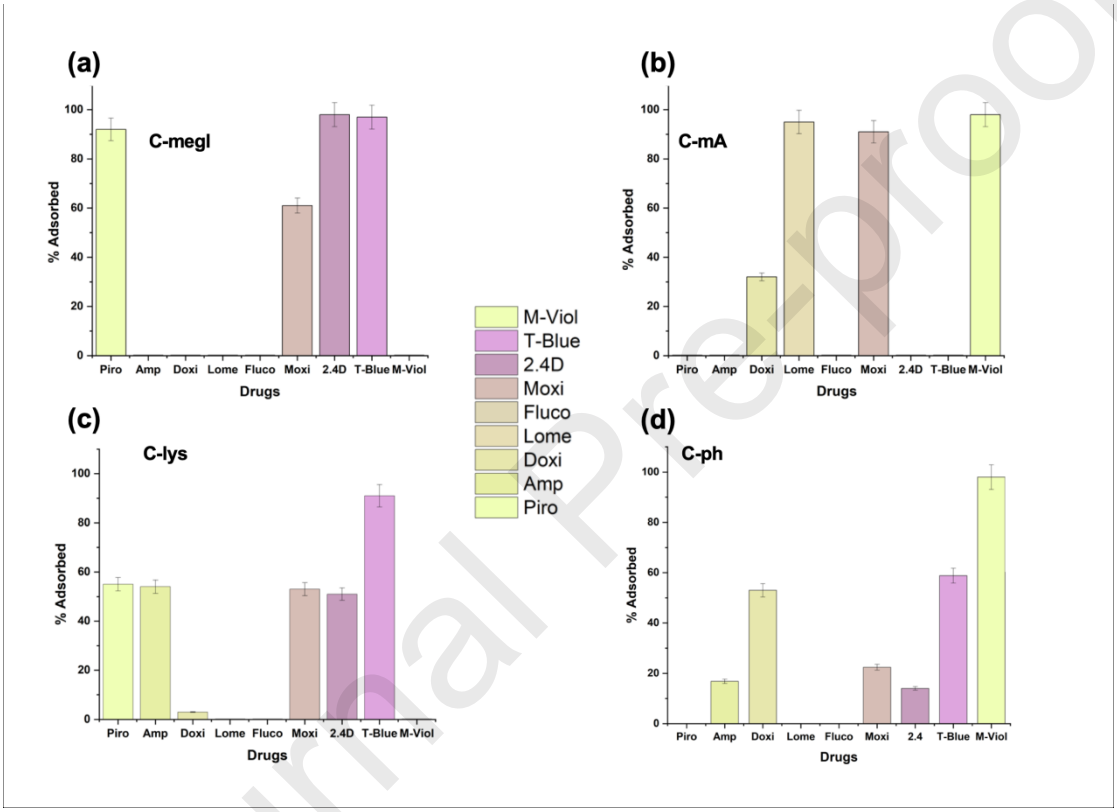


**Figure 3.** Percentage of adsorption of the target molecules starting from solutions of 25 ppm as a function of cryogels type. (a) C-megl, (b) C-mA. (c) C-lys, (d) C-ph.

Since C-lys is positively charged its performance is expected to be similar to that of C-megl. Indeed, if compared with the latter, C-lys adsorbs the same set of molecules (**Figure 3c**). It is worth emphasizing that the Lysine content within the sponge is only 25% whereas the remaining part was

constituted by HEMA. Thus, its chelating ability turns out to be much higher than the meglumine moieties constituting C-megl. Most importantly, C-lys revealed an affinity towards ampicillin sodium salt which is not detected for C-megl, and performance better than the one detected for C-ph. In this case, the lysine structure seems to play a key role in chelating such drugs by interactions including hydrogen bonding and/or Van der Walls, accomplished by steric factors that cannot be excluded. Indeed, we can speculate on a preferential affinity of Moxi versus the less bulky C-lys in forming H-bonds. Although highly relevant, the studies of other chemical/physical interactions among the adsorbate and adsorbent lie outside this work's scope.



Adsorption tests were also executed by using cryogel based on methacrylic acid (C-mA). The pKa of acrylic and methacrylic acid-based polymers is less than 5. This implies that the anchoring sites are deprotonated in this region and thus can attract positively charged molecules as also shown by the pHz reported in the S11.[43,46,56]

**Figure 3b** shows that this material can effectively remove positively charged molecules such as M-Viol and Lome molecules. Indeed, in its chlorohydrate formulation, Lome is positively charged at neutral and acid solution, thus allowing for the instauration of electrostatic interactions with the C-mA sites. Interestingly, up to 90% of Moxi was removed from the water. Sequestering may result from different and synergistic phenomena. Due to Moxi low solubility in water, pKa values may be used only in mathematical models.[57]

As to C-ph cryogel, excellent uptake values were registered for M-Viol. As reported by Fouzia Mashkoor *et al*.,[58] this property likely results from hydrogen bonds between the HEMA -OH group and the amine of M-Viol.

The adsorption tests carried out with all the cryogels showed that Fluco was not removed.

Taking advantage of their spongy properties, after the adsorption all samples can be squeezed to release decontaminated water, whilst the target molecules are trapped within the macroporous structures. Specifically, C-megl and C-mA were loaded with solutions containing 10 ppm of Piro and Lome, respectively, until they reached full swelling. Following the loading, cryogels were squeezed and the released water was analyzed.

UV-Vis data clearly show that the aqueous solution thus obtained did not contain detectable amounts of the target contaminants that remained instead adsorbed within the sponges.

Compression tests were also performed for all samples (**Figure S12**). As expected, all curves exhibited an elastic deformation region at low strain values followed by a nonlinear stage at compression values above 30%.[59,60] C-megl displayed slightly lower values of compressive stress

over the entire deformation range investigated if compared to other samples. Young's modulus values calculated from the elastic region (<20% strain) were found to be 12.5 ± 1.8 kPa (C-ph), 10.9 ± 0.5 kPa (C-ma), 10.7 ± 2.1 kPa (C-lys), and 11.7 ± 1.0 kPa (C-meg).



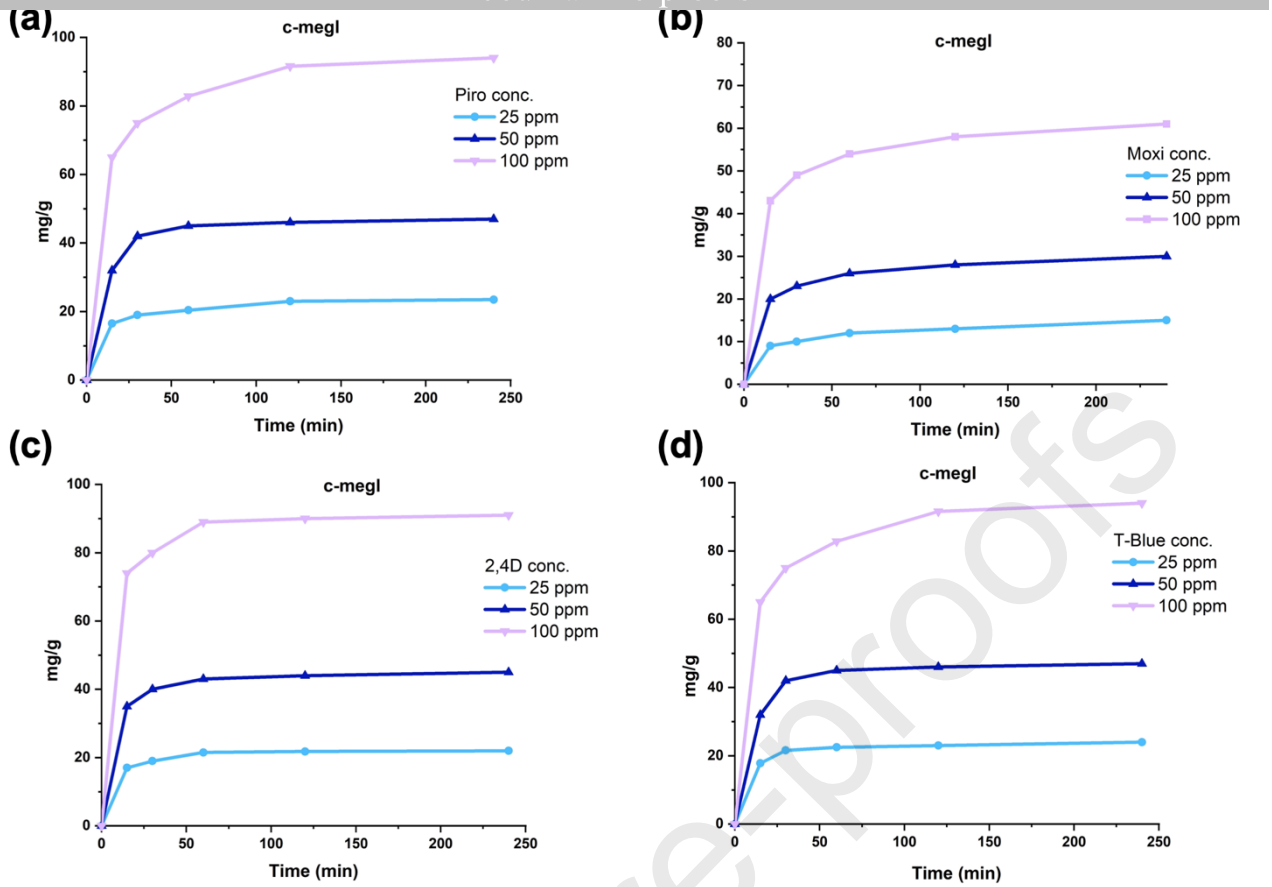


**Figure 4.** Adsorption studies of selected pollutants a) Piro, b) Moxi, c) 2,4D, d) T-Blue) at different concentration (25, 50, 100 ppm) and contact times with the C-megl cryogel.

Pollutants concentration effects of target molecules were also studied as a function of the contact times with cryogels (**Figures 4, and S9)**. About 4 mg of each material were immersed into the solutions performing the experiments in batch. **Figure 4** shows that, for all concentrations studied, 75% of contaminants adsorption took place within 15 min, reaching a plateau with higher immersion times. These experiments were used to evaluate the adsorption kinetics models governing the process. To this purpose, two different models (pseudo first and pseudo second order) were considered.

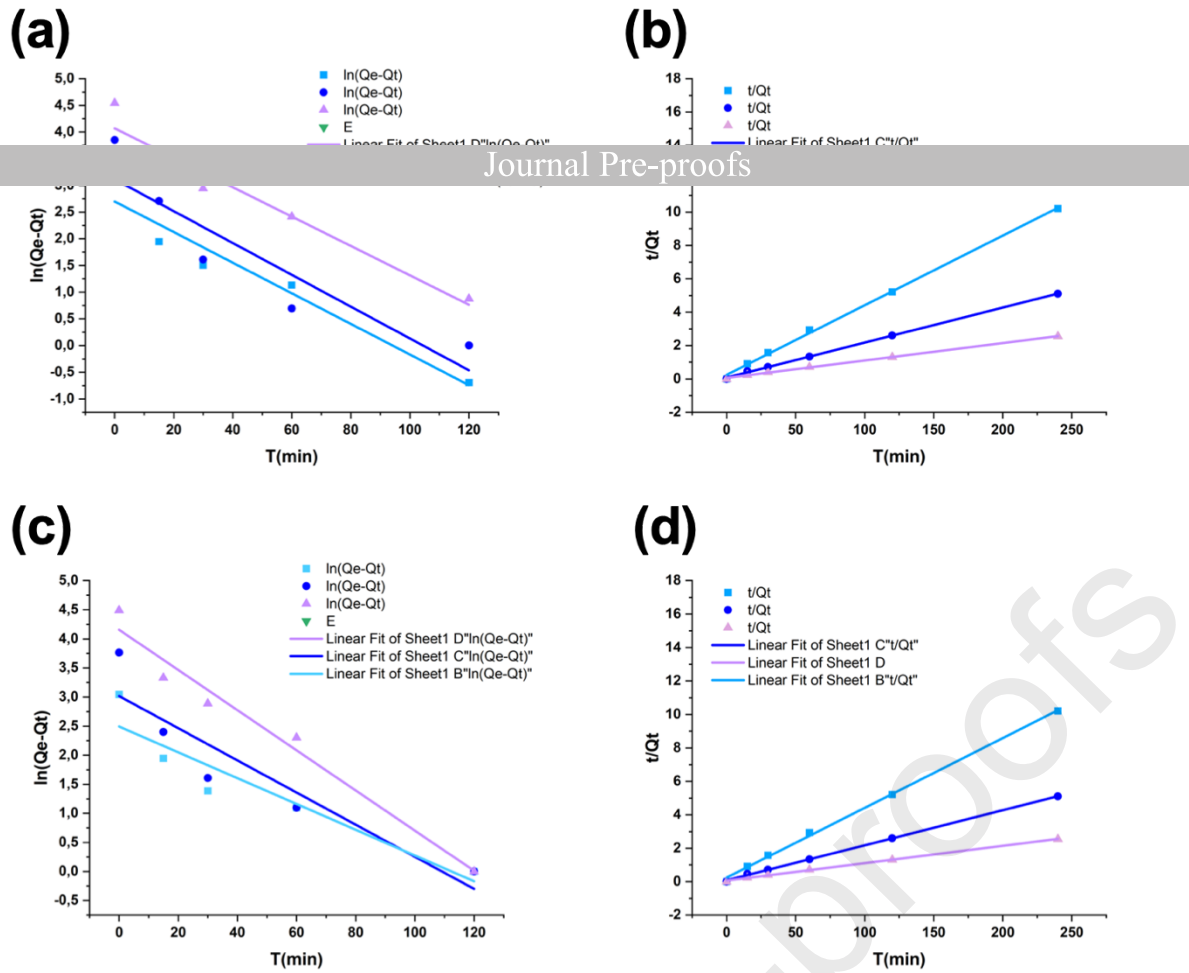


**Figure 5.** Adsorption kinetics models (pH: 6.5) of Piro for C-megl fitted with a) 1° order and b) 2° order and of Lome for C-mA fitted with c) 1° order and d) 2° order.

In the pseudo-first-order model developed by Lagergreen, the rate-limiting step involves only diffusion process, consequently the reaction rate depends only on the concentration of the adsorbed specie. For this reason, according to the pseudo-first-order kinetic model physisorption is the main adsorption mechanism. Lagergren's pseudo-first-order kinetic model for heterogeneous solid-liquid systems can be represented be the following formula:

$$lnln\,(Q_e - Q_t) = lnln\,Q_e - K_1\,t \qquad \textbf{(1)}$$

where $Q_e$ and $Q_t$ (mg/g) are the amounts of contaminants adsorbed at equilibrium and time t (min), respectively, assuming $Q_t$=0 at t = 0 as the initial condition. The adsorption equilibrium capacity ($Q_e$) may be calculated by the following equation

$$Q_e = \frac{(C_0 - C_e)x\,V}{W} \qquad \textbf{(2)}$$

where $C_0$ (mg/L) is the adsorbate initial concentration, Ce (mg $L^{-1}$) is the adsorbate concentration at the equilibrium, V (L) is the volume of water, W (g) is the weight of adsorbent used for the

adsorption experiment. Plotting $\ln(Q_e-Q_t)$ versus time (min) (Figure 5(a)), the slope value obtained through a linear data fitting allows estimating the constant rate $k_1$ ($min^{-1}$) for the adsorption process. In the pseudo-second-order kinetic model the adsorption mechanism is considered to be similar to a chemical reaction between the adsorbent and the adsorbate. Such process is commonly referred to as chemisorption. In these conditions, the adsorption capacity depends on the adsorbent rather than on the adsorbate concentration.[62,63]



The following equation can describe the pseudo-second-order model:

$$\frac{t}{Q_t} = \frac{1}{K_2 Q_e^2} + \frac{t}{Q_e} \qquad \textbf{(3)}$$

and allows for the calculation of the reaction rate $k_2$ (g $mg^{-1}min^{-1}$) and $Q_e$ by plotting the experimental data t/q versus t, where $Q_e$ and $k_2$ can be extrapolated from the slope and intercept of the best linear data fitting (**see Table 3** and Table S3).

**Table 3.** Kinetic parameters calculated from pseudo-first order, pseudo-second order $Q_e$, $K_1$ and $k_2$) extrapolated from plots in **Figure 5**.

| **a-b** | **Piro/ C-megl** | | |
|---|---|---|---|
| $C_0$ (mg $g^{-1}$) | 25 | 50 | 100 |
| $Q_{exp}$ (mg $g^{-1}$) | 23.5 | 47.1 | 94.2 |
| Pseudo I order | | | |
| $K_1$ ($min^{-1}$) | 0.029 | 0.030 | 0.028 |
| $Q_{eT}$ (mg $g^{-1}$) | 14.9 | 22.2 | 60.3 |
| $R^2$ | 0.942 | 0.839 | 0.943 |
| Pseudo II order | | | |
| $K_2$ x $10^{-3}$ ($min^{-1}$) | 7.2 | 5.7 | 1.8 |
| $Q_{eT}$ (mg $g^{-1}$) | 24.0 | 47.6 | 96.2 |
| $R^2$ | 0.998 | 0.999 | 0.999 |

| **c-d** | **Lome / C-mA** | | |
|---|---|---|---|
| $C_0$ (mg $g^{-1}$) | 25 | 50 | 100 |
| $Q_{exp}$ (mg $g^{-1}$) | 21.2 | 43.1 | 89.0 |
| Pseudo I order | | | |
| $K_1$ ($min^{-1}$) | 0.022 | 0.028 | 0.035 |
| $Q_{eT}$ (mg $g^{-1}$) | 12.1 | 24.0 | 63.9 |
| $R^2$ | 0.884 | 0.863 | 0.972 |
| Pseudo II order | | | |
| $K_2$ $10^{-3}$ ($min^{-1}$) | 7.0 | 6.3 | 1.9 |
| $Q_{eT}$ (mg $g^{-1}$) | 21.4 | 43.5 | 90.9 |
| $R^2$ | 0.998 | 0.999 | 0.999 |

As a result, the adsorption process for all materials and adsorbates used in this work is well represented by the pseudo-second-order kinetic model (Figure 5, Table S3 a-e). Indeed, the $R^2$ values of extrapolated curves indicated an excellent fit over the entire concentration range investigated.



The adsorption process can be represented as chemisorption in which strong intermolecular interactions (electrostatic or multiple hydrogen bonds) between the adsorbent and the adsorbate were involved. In particular, the protonated amine of C-megl at pH 6.5 attracted the negative charged Piro, whereas the -OH groups are likely responsible for hydrogen binding. Similarly, carboxylic groups drive the electrostatic interactions with Lome and other positively charged molecules. The significant divergence from the linearity from the pseudo-first-order model may result from the strong adsorption that takes place at the beginning of the process.

Their kinetic constants values obtained by fitting the experimental data sets are summarized in **Table 3.** It is worth emphasizing that $K_2$ values decreased as the concentration of the drug in the solution increased. This behavior likely indicates that a higher concentration of contaminant in solution might affect the adsorption process at the surface due to saturation phenomena.

From an industrial point of view, removing different types of organic or inorganic pollutants in a single step is an attractive option. In this context, we also tested the ability of one of the cryogels (C-megl) owing to its well-known ability to chelate metal oxyanions. Specifically, we focused our attention on the removal of arsenate and thymol blue from an aqueous solution having an initial concentration of these contaminants equal to 10 and 25 ppm, respectively.[40]

C-megl efficiently removes both contaminants, reducing their concentration in water to 3 ppb and 0.9 ppm for arsenic and thymol blue, respectively (**Figure S7**). As mentioned above, the material can be squeezed causing the release of decontaminated water whilst leaving both contaminants trapped within the sponge structure.

To further implement the range of material applicability in water remediation, a dual sponge was synthesized, taking advantage of the versatility of cryo-polymerization techniques.

Accordingly, a ‘dual’ sponge was obtained (see Experimental section) that allows for removing contaminants with acidic and basic properties. Specifically, C-megl was left in the reactor after the synthesis letting the reactant solutions to form the additional C-mA cryogel (see experimental section Figure 1).

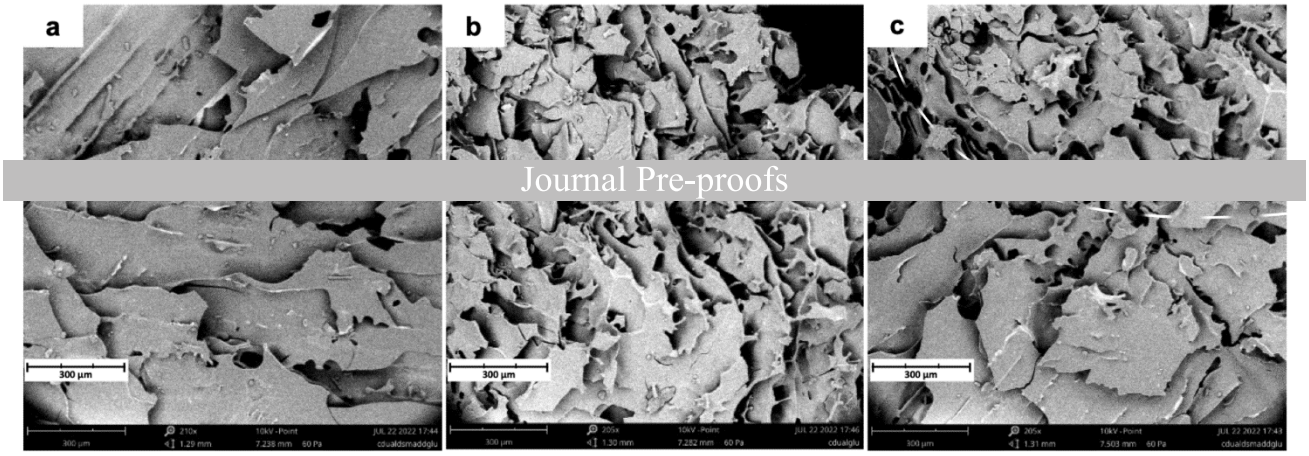




**Figure 6a-c.** SEM image (a) of the C-mA portion, (b) the C-Megl portion, and (c) their interface.

The SEM images of the 'dual' cryogel show that the procedure adopted results in a stable C-megl/C-mA linkage at the interface (**Figure 6c**). All micrographs exhibit a porosity change as described for the single cryogel (see **Figure 2**). The material exhibits continuous connections without revealing separation phases and/or cracks.

The 'dual' sponge **(Figure 7)** was kept in contact with the purple solution containing both dyes (T-Blue and M-viol) at a concentration of three ppm for 24 hours; after this period, the solution became colorless. The sponge regions consisting of C-megl and C-mA were colored in yellow and purple, respectively, evidencing the adsorption of both T-Blue and M-viol with a removal efficiency higher than 96% for both contaminants. It is worth highlighting that Qm calculated by Langmuir isotherms for T-Blu and M-Viol for each single sponge are 791.37 and 712.70 mg/g, respectively (**Figure S10 e Table S4**).

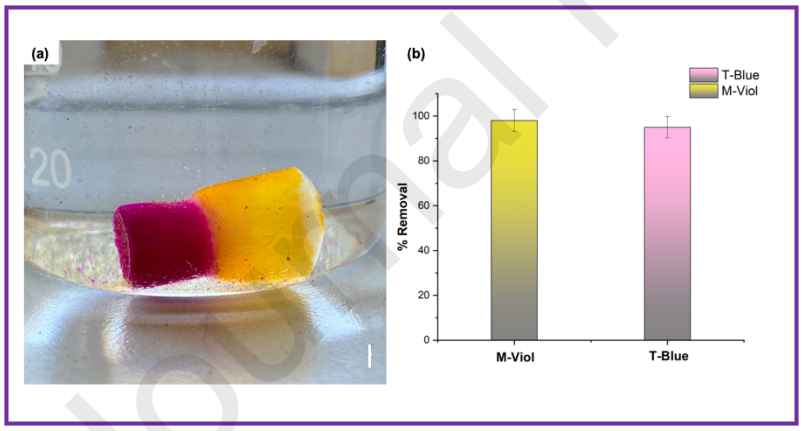


**Figure 7a-b. (a)** Dual sponge picture after dyes adsorption and **(b)** Removal efficiencies towards M-Viol and T-Blue after 24h of contact time

**RELEASE AND REGENERATION TESTS**

Such materials may also find applications as medical devices to release the selected pharmaceuticals under pH stimuli.



values of both the adsorbent and the adsorbate. Thus, for given adsorbents and adsorbates a change of pH after adsorption may result in the partial or total release of the drugs in the surrounding media. In case of a complete contaminant release, the cryogel is fully regenerated and ready to be used again as an adsorbent or to be loaded as a drug delivery system.

C-megl (≈10 mg) and C-lys (≈ 12 mg) were treated separately with a solution of 25 ppm of Piro until the adsorption plateau was reached. Similarly, two portions of C-mA (≈ 12 mg) were immersed in solutions of Lome or Doxi (25 ppm). Cryogels were removed from the 'contaminated' solutions, washed with water, and kept in clean water in the dark for seven days. Spectroscopical analyses showed that cryogels did not release the drug throughout the week. To demonstrate the ability in regenerate/release under pH stimuli, the sponges were re-immersed in solutions and the pH was adjusted to 3. Similarly, a set of experiments were carried out by immersing the cryogels in solutions at pH 4.5 and 9 and monitoring the drugs released from each cryogel over a 400 minute period. The acidic condition induced drugs release as a function of immersion times, as well as the nature of the cryogel and the drug load (**Figure 7**).

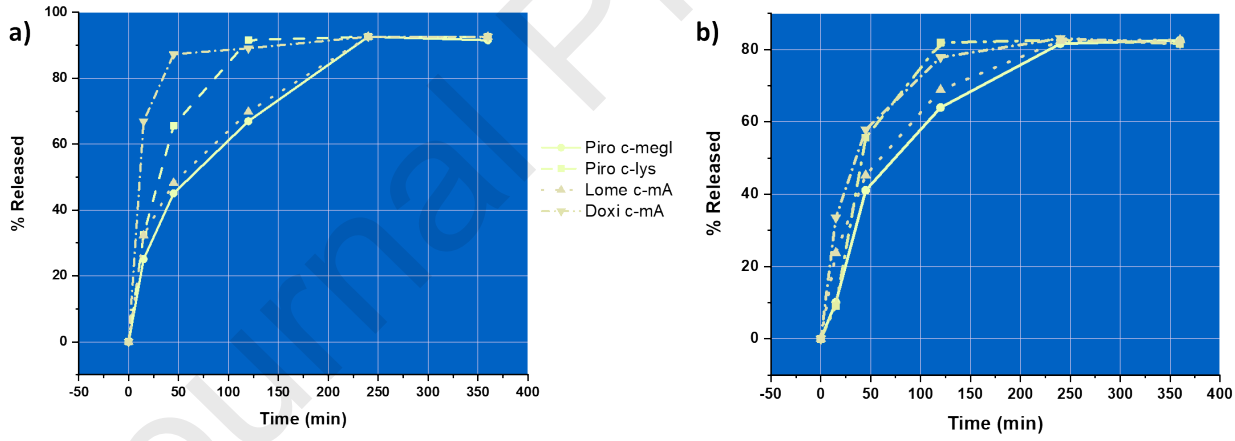


**Figure 7.** Cumulative releases of target pharmaceuticals as a function of immersion times at a) pH 3, b) pH 4.5.

Specifically, at pH 3, about 200 min were enough to find again *ca* 90% of the contaminant in water. As to C-megl and C-lys, low pH values the retention of the positively charged tertiary amine groups occurred. It may be reasonably assumed that the charge of Piro molecules changed from negative



For both C-megl and C-lys based sponges Piro was released more slowly than with other selected systems. This means that for these materials, a slower level of Piro release can be achieved by modulating the pH of the solution. Given that, higher pH values (Figure 7b) determined a slower Piro release. Only 18% of Piro was detected in solution at pH 4.5 after 30 min of soaking and reached 80% after 200 min. Piro could only be removed from the C-megl and C-lys using stronger acidic conditions (pH 1). At least five cycles of Piro adsorption were tested for the C-megl sponge without any significant loss of its sequestering capability (see experimental section and Fig S8). Regarding the release of Lome and Doxi, we are prone to consider that C-mA, played a key role in the desorption process. C-mA is mainly protonated at pH<5 (Fig S11) and this thwarts the electrostatic attraction towards positively charged molecules. At pH = 9, the desorption of Piro and Lome experienced different behavior. Indeed, both C-Megl and C-Lys at such pH are partially protonated. This status should involve a decrease in interactions with Piro molecules resulting in progressive release of the drugs. However, at pH 9 Piro remained negatively charged whereas the adsorbents positive sites are still enough to entrap the drug molecules. So, no release were registered.

Conversely, Lome was totally released from the C-mA due to the neutralization of the positive charges of the hydro-chlorohydrate drug formulation.

The regeneration of the 'dual' sponge was also achieved by following two different procedures. In the two-step method, the material was firstly soaked in a basic solution (≈pH 12) for 60 min. This time was enough to regenerate the C-megl part. After then, the sponge was washed with water and soaked again at pH 1. In this case, the regeneration of C-mA portion proceeded more slowly. Indeed, more than 150 min were needed to desorb the M-viol from the cryogel. Alternatively, a one-step washing method with ethanol can be used to remove both dyes simultaneously. Following such a procedure more than 90% of both dyes were removed from the treated materials in less than 30 min of immersion at room temperature.

## CONCLUSIONS

In this work, novel cryogel-based adsorbents were investigated to meet specific remediation needs arising from emerging contaminants in the industrial sectors.



This versatile platform of freestanding materials can be obtained by green chemical procedures since water may be used for polymerization and natural derivatives are selected as sequestering groups.

Similar to other hydrogel adsorbents, their use entails overwhelming advantages such as sustainable production, effective removal, and low energy consumption while in-service.

On the other hand, the macroporous morphologies whose forms and dimensions can be controlled with a low cost and easy procedure confer to cryogels additional benefits such us elasticity, limited pores obstruction, and fast diffusion pathways of the medium.

Based on the above, materials having both acid (C-mA), basic (C-lys and C-megl), and neutral (C-ph) functional groups were synthesized to remove a wide range of pharmaceuticals. It was demonstrated that every single cryogel possesses outstanding adsorption efficiencies towards target molecules having opposite charges. C-megl works efficiently up to a concentration of 100 ppm of Piro, 2,4 D and T-blue, eliminating more the 95% of molecules present in water. Similarly, C-mA can eliminate more than 90% of Lome, Moxi, and M-Viol at the same concentration and in presence of arsenate anions. Interestingly, the pHEMA cryogel functionalized with 25 % of lysine is the only material among those tested able to adsorb discrete amounts of ampicillin. Finally, a novel 'dual' sponge containing acid and basic sites was synthesized and used to effectively sequester antagonist species present in the same solution. Regeneration and releasing tests were performed by washing both C-megl and C-mA with acidic solutions. A tunable drug release was obtained, and the drug was entirely removed at pH 1.

The materials were tested up to five adsorption/regeneration cycles without a significant loss of efficiency. It is relevant to highlight that the production of materials that covers different markets can be economically advantageous from the industrial point of view.

**Acknowledgments**

This work was partially founded by ANTIBIO-Antibiotics Removal From Water By Imprinted Magnetic Nanomaterials project, ProgettidiRicerca@CNR call 2020 (CUP: B63C22000010005). The authors wish to thank Emanuele Francesco Mirabella (CNR-IPCB) for the technical assistance and prof. Giuseppe Arena for his valuable help in the Bronsted-Lowry equilibrium theory discussion.

## References



*Environ. Pollut.* **2014**, *187*, 193–201. https://doi.org/10.1016/j.envpol.2014.01.015.

(2) Jelic, A.; Gros, M.; Ginebreda, A.; Cespedes-Sánchez, R.; Ventura, F.; Petrovic, M.; Barcelo, D. Occurrence, Partition and Removal of Pharmaceuticals in Sewage Water and Sludge during Wastewater Treatment. *Water Res.* **2011**, *45* (3), 1165–1176. https://doi.org/10.1016/j.watres.2010.11.010.

(3) Guerra, P.; Kim, M.; Shah, A.; Alaee, M.; Smyth, S. A. Occurrence and Fate of Antibiotic, Analgesic/Anti-Inflammatory, and Antifungal Compounds in Five Wastewater Treatment Processes. *Sci. Total Environ.* **2014**, *473–474*, 235–243. https://doi.org/10.1016/j.scitotenv.2013.12.008.

(4) Von Sperling, M. *Wastewater Characteristics, Treatment and Disposal*; 2007. https://doi.org/10.2166/9781780402086.

(5) Bayabil, H. K.; Teshome, F. T.; Li, Y. C. Emerging Contaminants in Soil and Water. *Front. Environ. Sci.* **2022**, *10*, 1–8.

(6) Patel, M.; Kumar, R.; Kishor, K.; Mlsna, T.; Pittman, C. U.; Mohan, D. Pharmaceuticals of Emerging Concern in Aquatic Systems: Chemistry, Occurrence, Effects, and Removal Methods. *Chem. Rev.* **2019**, *119* (6), 3510–3673. https://doi.org/10.1021/acs.chemrev.8b00299.

(7) Kim, S.; Chu, K. H.; Al-Hamadani, Y. A. J.; Park, C. M.; Jang, M.; Kim, D.-H.; Yu, M.; Heo, J.; Yoon, Y. Removal of Contaminants of Emerging Concern by Membranes in Water and Wastewater: A Review. *Chem. Eng. J.* **2018**, *335*, 896–914. https://doi.org/10.1016/j.cej.2017.11.044.

(8) Rojas, S.; Horcajada, P. Metal–Organic Frameworks for the Removal of Emerging Organic Contaminants in Water. *Chem. Rev.* **2020**, *120* (16), 8378–8415. https://doi.org/10.1021/acs.chemrev.9b00797.

(9) Xu, Y.; Liu, T.; Zhang, Y.; Ge, F.; Steel, R. M.; Sun, L. Advances in Technologies for Pharmaceuticals and Personal Care Products Removal. *J. Mater. Chem. A* **2017**, *5* (24), 12001–12014. https://doi.org/10.1039/C7TA03698A.

(10) Cantarella, M.; Carroccio, S. C.; Dattilo, S.; Avolio, R.; Castaldo, R.; Puglisi, C.; Privitera, V. Molecularly Imprinted Polymer for Selective Adsorption of Diclofenac from Contaminated Water. *Chem. Eng. J.* **2019**, *367*, 180–188. https://doi.org/10.1016/j.cej.2019.02.146.

(11) Rathi, B. S.; Kumar, P. S.; Show, P.-L. A Review on Effective Removal of Emerging Contaminants from Aquatic Systems: Current Trends and Scope for Further Research. *J. Hazard. Mater.* **2021**, *409*, 124413. https://doi.org/10.1016/j.jhazmat.2020.124413.

(12) Ncibi, M. C.; Mahjoub, B.; Mahjoub, O.; Sillanpää, M. Remediation of Emerging Pollutants in Contaminated Wastewater and Aquatic Environments: Biomass-Based Technologies. *CLEAN – Soil Air Water* **2017**, *45* (5), 1700101. https://doi.org/10.1002/clen.201700101.

(13) Lin, H.; Chen, K.; Du, L.; Gao, P.; Zheng, J.; Liu, Y.; Ma, L. Efficient and Selective Adsorption of Methylene Blue and Methyl Violet Dyes by Yellow Passion Fruit Peel. *Environ. Technol.* **2021**, *0* (0), 1–12. https://doi.org/10.1080/09593330.2021.1924288.

(14) Khasawneh, O. F. S.; Palaniandy, P. Occurrence and Removal of Pharmaceuticals in Wastewater Treatment Plants. *Process Saf. Environ. Prot.* **2021**, *150*, 532–556. https://doi.org/10.1016/j.psep.2021.04.045

(15) Chimupala, Y.; Phromma, C.; Yimklan, S.; Semakul, N.; Ruankham, P. Dye Wastewater Treatment Enabled by Piezo-Enhanced Photocatalysis of Single-Component ZnO Nanoparticles. *RSC Adv.* **2020**, *10* (48), 28567–28575. https://doi.org/10.1039/D0RA04746E.

(16) Phoon, B. L.; Ong, C. C.; Mohamed Saheed, M. S.; Show, P.-L.; Chang, J.-S.; Ling, T. C.; Lam, S. S.; Juan, J. C. Conventional and Emerging Technologies for Removal of Antibiotics from

Wastewater. *J. Hazard. Mater.* **2020**, *400*, 122961. https://doi.org/10.1016/j.jhazmat.2020.122961.
(17) Riaz, L.; Mahmood, T.; Khalid, A.; Rashid, A.; Ahmed Siddique, M. B.; Kamal, A.; Coyne, M. S. Fluoroquinolones (FQs) in the Environment: A Review on Their Abundance, Sorption and Toxicity in Soil. *Chemosphere* **2018**, *191*, 704–720. https://doi.org/10.1016/j.chemosphere.2017.10.092.

(18) Guidi, L. R.; Santos, F. A.; Ribeiro, A. C. S. R.; Fernandes, C.; Silva, L. H. M.; Gloria, M. B. A. Quinolones and Tetracyclines in Aquaculture Fish by a Simple and Rapid LC-MS/MS Method. *Food Chem.* **2018**, *245*, 1232–1238. https://doi.org/10.1016/j.foodchem.2017.11.094.
(19) Shen, L.; Liu, Y.; Xu, H.-L. Treatment of Ampicillin-Loaded Wastewater by Combined Adsorption and Biodegradation. *J. Chem. Technol. Biotechnol.* **2010**, *85* (6), 814–820. https://doi.org/10.1002/jctb.2369.
(20) Aniagor, C. O.; Igwegbe, C. A.; Ighalo, J. O.; Oba, S. N. Adsorption of Doxycycline from Aqueous Media: A Review. *J. Mol. Liq.* **2021**, *334*, 116124. https://doi.org/10.1016/j.molliq.2021.116124.
(21) Mesa, L. M.; Hörler, J.; Lindt, I.; Gutiérrez, M. F.; Negro, L.; Mayora, G.; Montalto, L.; Ballent, M.; Lifschitz, A. Effects of the Antiparasitic Drug Moxidectin in Cattle Dung on Zooplankton and Benthic Invertebrates and Its Accumulation in a Water-Sediment System. *Arch. Environ. Contam. Toxicol.* **2018**, *75* (2), 316–326. https://doi.org/10.1007/s00244-018-0539-5.
(22) Muniz, M. S.; Halbach, K.; Alves Araruna, I. C.; Martins, R. X.; Seiwert, B.; Lechtenfeld, O.; Reemtsma, T.; Farias, D. Moxidectin Toxicity to Zebrafish Embryos: Bioaccumulation and Biomarker Responses. *Environ. Pollut.* **2021**, *283*, 117096. https://doi.org/10.1016/j.envpol.2021.117096.
(23) Frontistis, Z. Degradation of the Nonsteroidal Anti-Inflammatory Drug Piroxicam by Iron Activated Persulfate: The Role of Water Matrix and Ultrasound Synergy. *Int. J. Environ. Res. Public. Health* **2018**, *15* (11), 2600. https://doi.org/10.3390/ijerph15112600.
(24) Stathoulopoulos, A.; Mantzavinos, D.; Frontistis, Z. Coupling Persulfate-Based AOPs: A Novel Approach for Piroxicam Degradation in Aqueous Matrices. *Water* **2020**, *12* (6), 1530. https://doi.org/10.3390/w12061530.
(25) García-Valcárcel, A. I.; Tadeo, J. L. Influence of Moisture on the Availability and Persistence of Clotrimazole and Fluconazole in Sludge-Amended Soil. *Environ. Toxicol. Chem.* **2012**, *31* (3), 501–507. https://doi.org/10.1002/etc.1711.
(26) Coelho, E. R. C.; Brito, G. M. de; Frasson Loureiro, L.; Schettino, M. A.; Freitas, J. C. C. de. 2,4-Dichlorophenoxyacetic Acid (2,4-D) Micropollutant Herbicide Removing from Water Using Granular and Powdered Activated Carbons: A Comparison Applied for Water Treatment and Health Safety. *J. Environ. Sci. Health Part B* **2020**, *55* (4), 361–375. https://doi.org/10.1080/03601234.2019.1705113.
(27) Wang, Z.; Xue, M.; Huang, K.; Liu, Z. *Textile Dyeing Wastewater Treatment*; IntechOpen, 2011. https://doi.org/10.5772/22670.
(28) Li, J.; Mooney, D. J. Designing Hydrogels for Controlled Drug Delivery. *Nat. Rev. Mater.* **2016**, *1* (12), 1–17. https://doi.org/10.1038/natrevmats.2016.71.
(29) Rizzo, F.; Kehr, N. S. Recent Advances in Injectable Hydrogels for Controlled and Local Drug Delivery. *Adv. Healthc. Mater.* **2021**, *10* (1), 2001341. https://doi.org/10.1002/adhm.202001341.
(30) Liao, J.; Huang, H. Review on Magnetic Natural Polymer Constructed Hydrogels as Vehicles for Drug Delivery. *Biomacromolecules* **2020**, *21* (7), 2574–2594. https://doi.org/10.1021/acs.biomac.0c00566.
(31) García-González, C. A.; Budtova, T.; Durães, L.; Erkey, C.; Del Gaudio, P.; Gurikov, P.; Koebel, M.; Liebner, F.; Neagu, M.; Smirnova, I. An Opinion Paper on Aerogels for Biomedical and Environmental Applications. *Molecules* **2019**, *24* (9), 1815. https://doi.org/10.3390/molecules24091815.
(32) Franco, P.; Cardea, S.; Tabernero, A.; De Marco, I. Porous Aerogels and Adsorption of

Pollutants from Water and Air: A Review. *Molecules* **2021**, *26* (15), 4440. https://doi.org/10.3390/molecules26154440.
(33) Idumah, C. I.; Ezika, A. C.; Okpechi, V. U. Emerging Trends in Polymer Aerogel Nanoarchitectures, Surfaces, Interfaces and Applications. *Surf. Interfaces* **2021**, *25*, 101258. https://doi.org/10.1016/j.surfin.2021.101258.

(34) Cunsolo, F.; Mecca, T.; Spina, R. L.; Spitaleri, F. Cryogel for the Removal of Heparins and Heparinoids from Aqueous Solutions, Physiological Solutions and Biological Fluids, Preparation Process and Uses Thereof. WO2017137919A1, August 17, 2017.
(35) *Polymeric Cryogels*; Okay, O., Ed.; Advances in Polymer Science; Springer International Publishing: Cham, 2014; Vol. 263. https://doi.org/10.1007/978-3-319-05846-7.
(36) Cantarella, M.; Impellizzeri, G.; Di Mauro, A.; Privitera, V.; Carroccio, S. C. Innovative Polymeric Hybrid Nanocomposites for Application in Photocatalysis. *Polymers* **2021**, *13* (8), 1184. https://doi.org/10.3390/polym13081184.
(37) Kudaibergenov, S. E.; Tatykhanova, G. S.; Klivenko, A. N. Complexation of Macroporous Amphoteric Cryogels Based on N,N-Dimethylaminoethyl Methacrylate and Methacrylic Acid with Dyes, Surfactant, and Protein. *J. Appl. Polym. Sci.* **2016**, *133* (32). https://doi.org/10.1002/app.43784.
(38) Tekin, K.; Uzun, L.; Şahin, Ç. A.; Bektaş, S.; Denizli, A. Preparation and Characterization of Composite Cryogels Containing Imidazole Group and Use in Heavy Metal Removal. *React. Funct. Polym.* **2011**, *71* (10), 985–993. https://doi.org/10.1016/j.reactfunctpolym.2011.06.005.
(39) Mecca, T.; Ussia, M.; Caretti, D.; Cunsolo, F.; Dattilo, S.; Scurti, S.; Privitera, V.; Carroccio, S. C. N-Methyl-D-Glucamine Based Cryogels as Reusable Sponges to Enhance Heavy Metals Removal from Water. *Chem. Eng. J.* **2020**, *399*, 125753. https://doi.org/10.1016/j.cej.2020.125753.
(40) Türkmen, D.; Bakhshpour, M.; Akgönüllü, S.; Aşır, S.; Denizli, A. Heavy Metal Ions Removal From Wastewater Using Cryogels: A Review. *Front. Sustain.* **2022**, *3*, 1–17.
(41) Ussia, M.; Di Mauro, A.; Mecca, T.; Cunsolo, F.; Nicotra, G.; Spinella, C.; Cerruti, P.; Impellizzeri, G.; Privitera, V.; Carroccio, S. C. ZnO–PHEMA Nanocomposites: An Ecofriendly and Reusable Material for Water Remediation. *ACS Appl. Mater. Interfaces* **2018**, *10* (46), 40100–40110. https://doi.org/10.1021/acsami.8b13029.
(42) Spina, R. L.; Tripisciano, C.; Mecca, T.; Cunsolo, F.; Weber, V.; Mattiasson, B. Chemically Modified Poly(2-Hydroxyethyl Methacrylate) Cryogel for the Adsorption of Heparin. J. Biomed. Mater. Res. B Appl. Biomater. 2014, 102 (6), 1207–1216. https://doi.org/10.1002/jbm.b.33104.
(43) Sahiner, N.; Seven, F. The Use of Superporous p(AAc (Acrylic Acid)) Cryogels as Support for Co and Ni Nanoparticle Preparation and as Reactor in H2 Production from Sodium Borohydride Hydrolysis. *Energy* **2014**, *71*, 170–179. https://doi.org/10.1016/j.energy.2014.04.031.
(44) Conti, E.; Dattilo, S.; Costa, G.; Puglisi, C. Bioaccumulation of Trace Elements in the Sandhopper Talitrus Saltator (Montagu) from the Ionian Sandy Coasts of Sicily. *Ecotoxicol. Environ. Saf.* **2016**, *129*, 57–65. https://doi.org/10.1016/j.ecoenv.2016.03.008.
(45) Yuan, Z.; Wang, J.; Wang, Y.; Liu, Q.; Zhong, Y.; Wang, Y.; Li, L.; Lincoln, S. F.; Guo, X. Preparation of a Poly(Acrylic Acid) Based Hydrogel with Fast Adsorption Rate and High Adsorption Capacity for the Removal of Cationic Dyes. *RSC Adv.* **2019**, *9* (37), 21075–21085. https://doi.org/10.1039/C9RA03077H.
(46) Dickhaus, B. N.; Priefer, R. Determination of Polyelectrolyte PKa Values Using Surface-to-Air Tension Measurements. *Colloids Surf. Physicochem. Eng. Asp.* **2016**, *488*, 15–19. https://doi.org/10.1016/j.colsurfa.2015.10.015.
(47) Ibarra-Montaño, E. L.; Rodríguez-Laguna, N.; Sánchez-Hernández, A.; Rojas-Hernández, A. Determination of PKa Values for Acrylic, Methacrylic and Itaconic Acids by 1H and 13C NMR in Deuterated Water. *J. Appl. Solut. Chem. Model.* **2015**. https://doi.org/10.6000/1929-5030.2015.04.01.2.
(48) Gupta, N. V.; Shivakumar, H. Investigation of Swelling Behavior and Mechanical Properties of a PH-Sensitive Superporous Hydrogel Composite. *Iran. J. Pharm. Res. IJPR* **2012**, *11*, 481–493.
(49) Belaidi, O.; Adjim, M.; Bouchaour, T.; Maschke, U. FT-IR and FT-Raman Spectra of 2-

Hydroxyethyl Methacrylate--A Conformational and Vibrational Analysis. *Spectrochim. Acta. A. Mol. Biomol. Spectrosc.* **2015**, *148*, 396–404. https://doi.org/10.1016/j.saa.2015.03.101.
(50) Ebrahiminezhad, A.; Ghasemi, Y.; Rasoul-Amini, S.; Barar, J.; Davaran, S. Impact of Amino-Acid Coating on the Synthesis and Characteristics of Iron-Oxide Nanoparticles (IONs). *Bull. Korean Chem. Soc.* **2012**, *33* (12), 3957–3962. https://doi.org/10.5012/bkcs.2012.33.12.3957.

(51) Połowczyk, I.; Urbano, B. F.; Rivas, B. L.; Bryjak, M.; Kabay, N. Equilibrium and Kinetic Study of Chromium Sorption on Resins with Quaternary Ammonium and N-Methyl-d-Glucamine Groups. *Chem. Eng. J.* **2016**, *284*, 395–404. https://doi.org/10.1016/j.cej.2015.09.018.
(52) Scurti, S.; Dattilo, S.; Gintsburg, D.; Vigliotti, L.; Winkler, A.; Carroccio, S. C.; Caretti, D. Superparamagnetic Iron Oxide Nanoparticle Nanodevices Based on Fe3O4 Coated by Megluminic Ligands for the Adsorption of Metal Anions from Water. *ACS Omega* **2022**, *7* (12), 10775–10788. https://doi.org/10.1021/acsomega.2c00558.
(53) Çelebİer, M.; Nennİ, M.; Kaplan, O.; Akgeyİk, E.; Kaynak, M. S.; Şahİn, S. Determination of the Physicochemical Properties of Piroxicam. *Turk. J. Pharm. Sci.* **2020**, *17* (5), 535–541. https://doi.org/10.4274/tjps.galenos.2019.82335.
(54) Shimada, T.; Tochinai, K.; Hasegawa, T. Determination of PH Dependent Structures of Thymol Blue Revealed by Cooperative Analytical Method of Quantum Chemistry and Multivariate Analysis of Electronic Absorption Spectra. *Bull. Chem. Soc. Jpn.* **2019**, *92* (10), 1759–1766. https://doi.org/10.1246/bcsj.20190118.
(55) Vieira, T.; Becegato, V. A.; Paulino, A. T. Equilibrium Isotherms, Kinetics, and Thermodynamics of the Adsorption of 2,4-Dichlorophenoxyacetic Acid to Chitosan-Based Hydrogels. *Water. Air. Soil Pollut.* **2021**, *232* (2), 60. https://doi.org/10.1007/s11270-021-05021-6.
(56) Sorribes-Soriano, A.; Armenta, S.; Turrillas, F. A. E.-; Herrero-Martínez, J. M. Tuning the Selectivity of Molecularly Imprinted Polymer Extraction of Arylcyclohexylamines: From Class-Selective to Specific. *Anal. Chim. Acta* **2020,** *1124*, 94–103. https://doi.org/10.1016/j.aca.2020.05.035.
(57) *Moxidectin*. https://go.drugbank.com/drugs/DB11431 (accessed 2022-08-25).
(58) Mashkoor, F.; Nasar, A.; Inamuddin; Asiri, A. M. Exploring the Reusability of Synthetically Contaminated Wastewater Containing Crystal Violet Dye Using Tectona Grandis Sawdust as a Very Low-Cost Adsorbent. *Sci. Rep.* **2018**, *8* (1), 8314. https://doi.org/10.1038/s41598-018-26655-3.
(59) Wan, B.; Li, J.; Ma, F.; Yu, N.; Zhang, W.; Jiang, L.; Wei, H. Preparation and Properties of Cryogel Based on Poly(2-Hydroxyethyl Methacrylate-Co-Glycidyl Methacrylate). *Langmuir* **2019**, *35* (9), 3284–3294. https://doi.org/10.1021/acs.langmuir.8b04021.
(60) Kumari, J.; Kumar, A. Development of Polymer Based Cryogel Matrix for Transportation and Storage of Mammalian Cells. *Sci. Rep.* **2017**, *7* (1), 41551. https://doi.org/10.1038/srep41551.
(61) Ho, Y. S.; McKay, G. Pseudo-Second Order Model for Sorption Processes. *Process Biochem.* **1999**, *34* (5), 451–465. https://doi.org/10.1016/S0032-9592(98)00112-5.
(62) Alberti, G.; Amendola, V.; Pesavento, M.; Biesuz, R. Beyond the Synthesis of Novel Solid Phases: Review on Modelling of Sorption Phenomena. *Coord. Chem. Rev.* **2012**, *256* (1), 28–45. https://doi.org/10.1016/j.ccr.2011.08.022.
(63) Robati, D. Pseudo-Second-Order Kinetic Equations for Modeling Adsorption Systems for Removal of Lead Ions Using Multi-Walled Carbon Nanotube. *J. Nanostructure Chem.* **2013**, *3* (1), 55. https://doi.org/10.1186/2193-8865-3-55.
(64) Chenthamara, D.; Ramakrishnan, S. G.; Robert, B.; Murugan, P.; Subramaniam, S. Zinc Chloride Activated Carbon from Pleurotus Floridanus Biomass for Piroxicam Adsorption. *J. Chem. Technol. Biotechnol.* **2022**, *97* (3), 719–730. https://doi.org/10.1002/jctb.6957.

**Declaration of interests**

☐ The authors declare that they have no known competing financial interests or personal relationships that could have appeared to influence the work reported in this paper.



☒ The authors declare the following financial interests/personal relationships which may be considered as potential competing interests:

Sabrina Carola Carroccio reports was provided by Italian National Reaserch Council. Sabrina Carola Carroccio has patent pending to CNR- PCT/EP2020/069695 (WO2021013596A1). Tommaso Mecca has patent pending to CNR-WO2017137919A1.




- New dual cryogel were designed by using cryo-polymerization.
- Macroporous structures provide an remarkable complexation of emerging pollutant in water.
- Pharmaceutical sorption capacity and release can be tuned by changing pH.
- The material can be regenerated and reused preserving its uptake efficiency.